International Journal of Progressive Sciences and Technologies (IJPSAT)
ISSN: 2509-0119.

Vol. 32 No. 1 April 2022, pp. 222-249

Power consumption reduction on RADAR MIMO using Lift Wavelet Transform – Filter Bank based MultiCarrier (LWT-FBMC)

Marie Emile RANDRIANANDRASANA[1], Paul Auguste RANDRIAMITANTSOA[2], Andry Auguste RANDRIAMITANTSOA[3]

[1]Department of Telecommunication, Antsirabe Vankinankaratra High Education Institute, Antsirabe Vankinankaratra, emile3marie@gmail.com

[2]Department of Telecommunication, High School Polytechnic of Antananarivo, Anosizato, Antananarivo, rpauguste@gmail.com

[3]Department of Telecommunication, High School Polytechnic of Antananarivo, Anosizato, Antananarivo, andriau23@gmail.com

***Abstract*— The RADAR MIMO uses multiple antennas on emitter and receiver for avoiding doppler effects, improving the robustness of binary error of transmission. Multi carrier modulation is introduced to have good performance about doppler effects like Filter Bank based MultiCarrier (FBMC) used specially on 5G. It is a multicarrier modulation like Orthogonal Frequency Division Multiplex (OFDM) but each carrier is processed with filter bank to reduce the outside band of spectrum. The problems of OFDM and FBMC are concerned about Discret Fourier Transform (DFT) which gives Peak Average Power Ratio (PAPR) and high time processing. This article replaces the DFT by Discret Cosine Transform (DCT) and Lift Wavelet Transform (LWT). I also noticed that the LWT-FBMC is a proposition on 6G modulations and FFT is the same function as DFT. The difference is that FFT uses rapid multiplication instead of simple multiplication.**

This study presents the difference between RADAR MIMO OFDM and RADAR MIMO FBMC. We did a simulation on Matlab about the RADAR MIMO FBMC using multiple transformations like DFT, DCT and LWT and compared the results (Power Average Power Ration or PAPR, Bit Error Ratio or BER) on each methods. We present all mathematics formulas with simplified diagrams and evaluate the time complexity of each method.

As a result, we can deduce that time consumption for LWT is much lower than DCT and DFT. This method doesn't use exponential calculations but just addition and substraction formula. The LWT also presents a lower PAPR but has a larger BER. So, LWT-FBMC presents a good performance in reduction of power consumption on RADAR MIMO instead of classic DCT or DFT FBMC.

Keywords*— *RADAR, DCT, LWT, MIMO, FBMC

I. INTRODUCTION

Let's a MIMO radar system colocate N_t emitter antenna and N_r receiver antenna. Let $S_m \in \mathbb{C}^L$, the wave on discret time which should be transmitted. Let $S = [s_1, s_2, \dots, s_{N_t}]^T \in \mathbb{C}^{N_t \times L}$, the matrix of emitter waves where L will be the wavelength. Knowing that, the radar emits M impulsions in the interval of coherent treatment with the frequency f_r.

1.1 Target

The target catches signal coming to the emitter and sends this signal. The signal could be expressed by the equation (1) :

$$Y_{t,m} = \beta_t . exp^{j(m-1)\omega_t} a_r(\theta_t) a_t^T(\theta_t) s \quad (1)$$

Where,

$a_t(\theta_t) = [\,1, \dots,\ e^{j(N_t-1)\pi d_t sin\theta_t}]^T$: the vector director of the antenna emitter

$a_r(\theta_t) = [\,1, \dots,\ e^{j(N_r-1)\pi d_r sin\theta_t}]^T$: the vector director of the antenna receiver.

θ_t : the target's direction of arrival

β_t : the signal's amplitude

$\omega_t = 2\pi f_t, f_t$: the doppler frequency of a normalized target.

1.2 First model of received signal

The MIMO radar will be composed by n_T emitter antenna and N_r receiver antenna.

A series of independent signals are transmitted in a logical manner by each transmitting element. Propagation of a signal from a transmitting element to a receiving element results in propagation through a channel with three (03) components:

- a channel of the propagation to the target
- a reflective target
- a channel reverses to the receiving probe.

The two channels will be jointly parameterized by a parametric model, from the parameter $\mathfrak{r}$.

The target is considered to be specific, in other words, the physical dimensions of the target are rather small, which only turns out to be a point with the eyes of the radar. However, it is possible to consider the target as consisting of several reflecting centers.

For each transmit/receive transmission chain pair, the target response is approximated with a value to follow a random process. The equation (2) is a received signal model, due to a series of transmitted waveforms, a point target of the response vector a and a parametric channel model of $\mathfrak{r}$.

$$y = \begin{bmatrix} S(\mathfrak{r},1) & 0 \cdots & 0 \\ 0 & S(\mathfrak{r},2) & \vdots \\ . & . & \\ 0 & 0 \cdots & S(\mathfrak{r},n_R) \end{bmatrix} \begin{bmatrix} a_1 \\ a_2 \\ . \\ a_{n_R} \end{bmatrix} + \begin{bmatrix} n_1 \\ n_2 \\ . \\ n_{n_R} \end{bmatrix} \quad (2)$$

Let $e_k(t)$ the respective impulse response of k different target.

$$e_k(t) = \sum_{r_f=1}^{R_f} m_{r_f}^{(k)} \delta\left(t - \tau_{r_f}^{(k)}\right) \quad (3)$$

Where,

$m_{r_f}^{(k)}$ and $\tau_{r_f}^{(k)}$: the magnitudes of the response for each repair center r_f and the time delay.

The transmitted waveforms $o_i(t)$ are also normalized to unity energy with energy levels defined by p_i for all $i \in [1, \cdots, T]$. Each waveform is multiplied by a beamforming vector $u_i \in \mathbb{C}^{N_T X1}$ to focus on the transmitted waveforms on the radar scene.

Thus, the transmitted radar MIMO signal represents a linear combination of the totality of all beams of the transmitted and associated waves at similar energy levels. It will be expressed by the equation (4).

$$o(t) = \sum_{i=1}^{T} u_i s_i \sqrt{p_i} \quad (4)$$

Losses or pathloss in free space are expressed by $l_T^{(k)}$ and $l_R^{(k)}$ for transmitting and receiving paths relating to each k individual target of the respective radar. Since each target is at the azimuth angle $\mathfrak{h}_K$ relative to the transmission row, the reflected signal of the k-th target can be defined as :

$$y_k(t) = e_k(t) * \left[\beta_T^H(\mathfrak{h}_k) o(t) l_T^{(k)}\right], k = 1, \dots, K, \quad (5)$$

Where,

$\beta_T(\mathfrak{h}_K) \in \mathbb{C}^{N_T X1}$: vector of various ranges in the direction of the target

(*) : the convolution operator

$(.)^H$: Hermitian or the complex transpose operator

When the reflected signal is received by the RADAR MIMO receiver, the received signal is expressed as the equation (6) :

$$z_r(t) = \sum_{k=1}^{K} \sum_{i=1}^{T} \alpha_{ri}^{(k)} [e_k(t) * o_i(t)] \sqrt{p_i} + \sum_{e=1}^{C_s} \sum_{i=1}^{T} \mu_{ri}^{(e)} [e_e(t) * o_i(t)] \sqrt{p_i} + v_r^H \eta(t) \quad (6)$$

Where,

$\beta_R(\theta_k) \in \mathbb{C}^{N_R X1}$: the vector director of various ranges of reception antenna of the azimuth direction

$\theta_k, \alpha_{ri}^{(k)} = l_R^{(k)} v_r^H \beta_R(\theta_k) \beta_T^H(\mathfrak{h}_k) y_k l_T^{(k)}$: reflexion coefficient

$e = 1, \dots, c_s$: source of clutter

The coefficients of periodic reflection and complexes of "clutter" $\mu_{ri}^{(e)}$ is defined by $\alpha_{ri}^{(k)}$ for the target radar with $\mu_{ri}^{(e)} = \tilde{l}_R^{(k)} v_r^H \tilde{\beta}_R(\tilde{\theta}_e) \beta_T^H(\tilde{\mathfrak{h}}_e) y_k \tilde{l}_T^{(k)}$.

Note that, $\mu_{ri}^{(e)}, \tilde{l}_R^{(k)}$ and $\tilde{l}_T^{(k)}$ define the pathloss coefficients corresponding to each source and “clutter” for the transmission and receiving paths, respectively.

The coefficient $\tilde{\mathfrak{h}}_e$ and $\tilde{\theta}_e$indicates the azimuths at which each source of "clutter" is produced relative to the transmission and receiving ranges, respectively.

1.3 Second model of received signal

In this second theory, Uniform Linear Antenna (ULA) uses a vector director to beam the signal in a specific direction. The signal to be transmitted is defined by the equation (7) :

$$x(m) = [x_1(m)\ x_2(m) \dots . x_{n_T}(m)] \quad (7)$$

$x_n(m)$: the bandbase signal of the m-ith emission element at the time index m.

The target with (his emplacement θ_k) receives the signal expressed by :

$$r_k(m) = \sum_{n=1}^{n_T} e^{-j(n-1)\pi \sin\theta_k} x_n(m), with, k = 1,2, \dots K \quad (8)$$

$$r_k(m) = a^H(\theta_k) x(m) \quad (9)$$

Where : $a(\theta_k)$ is the vector director defined by :

$$a(\theta_k) = [\,1\ \ e^{j\pi \sin\theta_k}\ \ e^{j2\pi \sin\theta_k} \dots \dots . e^{j(n_T-1)\pi \sin\theta_k}] \quad (10)$$

II. Material And Methods

2.1. Advanced Muti-carrier modulation

In OFDM the entire bandwidth is divided into a number of sub-carriers and these sub-carriers are transmitted in parallel to increase symbol duration to achieve high data rates; it is shown in fig. 1. An OFDM signal is the sum of all sub-carriers signal which are modulated at the sub channels of equal bandwidth.

To reduce Out of Band (OOB) on spectrum, advanced new filter give other advanced modulations like Universal Filtered Multicarrier (UFMC) and Filter Bank based MultiCarrier (FBMC).

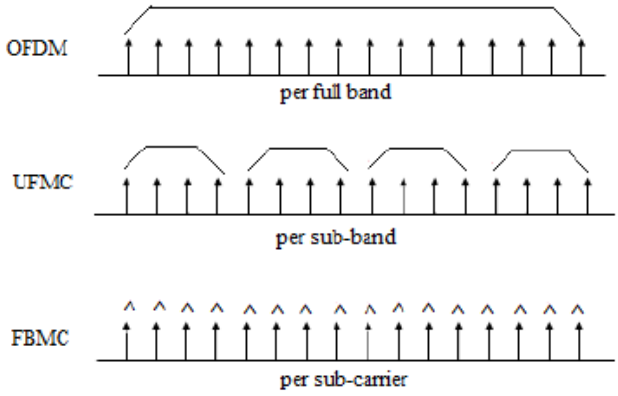

Fig. 1. *Filtering methods in OFDM, UFMC and FBMC*

2.2. Offset of Quadrature Amplitude Modulation (OQAM) on advanced modulation

The techniques of OQAM is based on two principles :

- On the emitter, the OQAM preprocessing
- On the receiver, the OQAM postprocessing

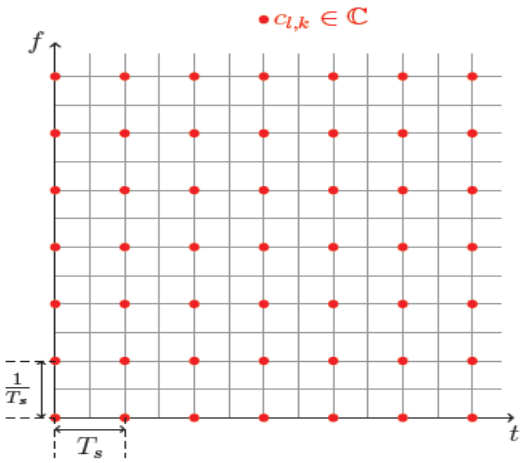

Fig. 2. *Time latency with QAM*

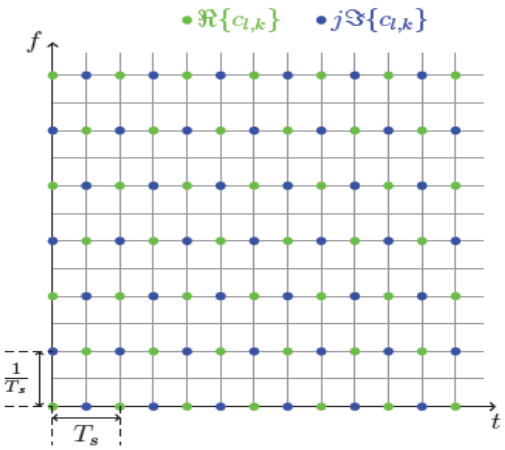

Fig. 3. *Time latency with O-QAM*

The first operation in the pre-processing block is the complex/real conversion. Indeed, instead of sending complex symbols (QAM symbols). The fig. 2 and 3 show the difference between time latency using QAM processing and OQAM processing with advanced modulation. The constant k and l represent the temporal index and the frequency index, respectively.

The objectives of OQAM are:

- Two symbols on the same carrier must be successively real and purely imaginary.
- In addition, the adjacent symbols between the two under carrier must also be successively real and purely imaginary.

Let $C_{l,k}$ the complex symbols that after OQAM modulation will become real symbols $a_{l,k}$ expressed by the equation (11). Recall that k is the temporal index and the frequent index.

$$a_{l,k} = \begin{cases} \boldsymbol{Real(C_{l,k})\ si\ l\ \ pair\ et\ k\ pair} \\ \boldsymbol{Imag(C_{l,k})\ si\ l\ impair\ et\ k\ pair} \\ \boldsymbol{Imag(C_{l,k})\ si\ l\ pair\ et\ k\ impair} \\ \boldsymbol{Real(C_{l,k})\ si\ l\ \ impair\ et\ k\ impair} \end{cases} \tag{11}$$

The second operation of the OQAM pre-processing block is a multiplication by:

$\theta_{l,k} = j^{l+k}$.

The symbols at the exit of the OQAM pre-processing block will modulate the carrie and which notes $X_{l,k}$ like on expression :

$$\boldsymbol{X_{l,k}(t) = \sum_{k=-\infty}^{+\infty} \theta_{l,k}.a_{l,k}.\delta(t - k\frac{T_s}{2})} \tag{12}$$

Where,

$\delta(t)$: impulsion of Dirac

The first operation of the OQAM post-processing block is multiplication by $\theta^*_{l,k}$ which is a conjugate complex of $\theta_{l,k}$. Then, there is a real/complex conversion. Indeed, two real symbols successively on a carrier form a complex symbol. The equation (13) gives the expression of complex symbols on the carrier l after OQAM post-processing.

$$C_{l,k} = \begin{cases} a_{l,k} + a_{l,k+1} \ \ si\ l\ pair\ et\ k\ pair \\ a_{l,k+1} + a_{l,k}\ si\ l\ impair\ et\ k\ pair \\ a_{l,k-1} + a_{l,k} \ \ si\ l\ pair\ et\ k\ impair \\ a_{l,k} + a_{l,k-1} \ \ si\ l\ impair\ et\ k\ impair \end{cases}$$

(13)

2.3. OFDM-OQAM MIMO radar

In MIMO radar system with M transmitter antennas and N receiver antennas, the transmitters are placed parallel to the axis of the abscesses are its antennas are spaced a distance dt, as the coordination of the same meter antenna is expressed by the equation (14).

$$E_m = E_0 + m.d_t.x. \tag{14}$$

Where, m= 0,… ,M-1 and $E_0 = \left[x_{t,0}, y_{t,0}, z_{t,0}\right]^T$

the first transmitter is located in the center O(0,0,0) and et $x = [1,0,0]^T$ is the unitary vector on the axis of x. Similar, the receivers are parallel to the order axis, they are spaced a distance d_r, n-ith receiver antenna are located on coordinate by the equation (15) :

$$R_n = R_0 + n.d_r.y, \tag{15}$$

Where, $R_0 = \left[x_{r,0}, y_{r,0}, z_{r,0}\right]^T$ and $y = [0,1,0]^T$

Each element in a transmitter system transmits a signal modulated in OFDM at an initial carrier frequency f_0. The base band OFDM signal consists of N sub-carrier frequencies with a uniformly spaced frequency Δf; the total bandwidth is expressed by the equation (16).

$$B\omega = N.\Delta f \tag{16}$$

The n-ith sub-carrier is modulated with a K-ith code sequence and it will be formulated by the equation (17) and the code should respect the orthogonal waveform condition :

$$c_{n,p} = \left[b_{n,p}^{(0)}, \dots, b_{n,p}^{(K-1)}\right]^T \tag{17}$$

Where, $c_{n,p}^H c_{n,p} = \begin{cases} 1, & p = p' \\ 0, & p \neq p' \end{cases}$

So, $c_n = \left[c_{n,0}, \dots, c_{n,P-1}\right] \in \mathbb{C}^{K \times P}$ and the expression could be rewrited like :

$$c_n^H c_n = I_n$$

The bit length t_b respects the orthogonality condition $t_b.\Delta f = 1$. The m-ith impulsion on the baseband OFDM could be expressed by the equation (18).

$$u_m(t) = \sum_{n=0}^{N-1} \sum_{k=0}^{K-1} b_{n,m}^{(k)} exp^{\{j2\pi t \Delta f (t-(k+1))t_c\}} rect\left(\frac{t - kt_s}{t_s} - \frac{1}{2}\right)$$

(18)

With,

$t_s = t_b - t_c$: symbol duration

$t_c = \propto t_b$: cyclic prefix duration

m = 0,…,P-1

$rect(t) = \begin{cases} 1, & \frac{-1}{2} \leq t < \frac{1}{2} \\ 0, & ailleurs \end{cases}$: rectangular signal

The baseband signal $u_m(t)$ is modulated with an initial carrier frequency f_0 for transmitting.

A target set is composed of the scattered ideal points I. The coordinate of i-th dispersed point is expressed by :

$$D_i = [x_i, y_i, z_t]^T \tag{19}$$

The amplitude of the relative dispersion is σ_i, which is a constant within an OFDM pulse width and for multiple transmitter/receiver channels.

The target velocity is fully estimated and compensated after pre-processing. The Doppler effect is negligible in all echo models as expressed by the equation (20):

$$t = \tau_{min} + kt_s + t_c + t_0, \tag{20}$$

With,

τ_{min} : being the beginning of a sample

$t_0 \in [0, t_b]$: initial time

The time interval of a (p,q)-th transmit/receive chain and i-th scatter is expressed by the equation (21).

$$\tau_{p,q}^{(i)} = \frac{\left(\|D_i - t_p\| + \|R_q - S_i\|\right)}{C} - \tau_{min} \tag{21}$$

Where,

c : the speed of light

The echo after the downlink is expressed by the equation (22).

$$s_q^{(k)}(t_0) = \sum_{p=0}^{P-1} \sum_{i=1}^{I} \sigma_i exp^{(-j2\pi f_0 \tau_{p,q}^{(i)}} \sum_{n=0}^{N-1} exp^{\{i2\pi \Delta f (t_0 - \tau_{p,q}^{(i)}\}} \sum_{k'=0}^{K-1} b_{n,p}^{(k')}$$
$$rect\left(\frac{(k-k')t_s + t_c + t_0 - \tau_{p,q}^{(i)}}{t_s} - \frac{1}{2}\right) + \vartheta_q^{(k)}(t_0) \tag{22}$$

Where,

$\vartheta_q^{(k)}(t_0)$: the noise

and $rect\left(\frac{(k-k')t_s+t_c+t_0-\tau_{p,q}^{(i)}}{t_s} - \frac{1}{2}\right) = \delta(k-k')$; $\delta(.)$ is an impulse function.

For the following, the processing methods will be described.

For q-th element received, and for k-th OFDM bit, the DFT calculation follows the sample index at a fast time. The echo in a frequency domain is written by the equation (23).

$$x_{n,q}^{(k)} = \frac{1}{N}\sum_{n=0}^{N-1} exp^{\left(j2\pi\frac{nl}{N}\right)} s_{lq}^{(k)} = \sum_{i=0}^{I} \sigma_i exp^{\{-j2\pi(n\Delta f+f_0)\tau_{p,q}^{(i)}\}} \sum_{p=0}^{P-1} b_{n,p}^{(k)} + V_{lq}^{(k)} \quad (23)$$

Where,

$x_{n,q}^{(k)}$: the n-th point results of the DFT and the echo in a frequency domain with n-th subcarrier

$V_{lq}^{(k)}$: the noise

N sub-carriers are separated without inter-carrier interference but the echoes received in P transmitting antennas are multiplexed and named serial to parallel.

To separate the transmitter and decode the sub-carriers, each sub-carrier is indexed n, we stack the DFT results of the K bits in a column vector :

$$s_{n,q} = \left[S_{n,q}^{(0)}, \dots, S_{n,q}^{(K-1)}\right]^T \quad (24)$$

Let,

$$s_{n,q} = C_n E_{n,q}\sigma + v_{n,q} \in \mathbb{C}^{K\times 1} \quad (25)$$

Where,

$C_n \in \mathbb{C}^{K\times P}$ and $E_{n,q}$: complex matrix with dimension $P \times I$

$\varepsilon_{n,p,q}^{(i)} = exp^{\{-j2\pi(n\Delta f+f_0)\tau_{p,q}^{(i)}\}}$: element of matrix C_n and the response of i-th disperser to n-th subcarrier for (p,q)-the transmitter/receiver chain.

$\sigma = [\sigma_1, \dots, \sigma_i]^T$: dispersion coefficient

$v_{n,q} = \left[V_{n,q}^{(0)}, \dots, V_{n,q}^{(K-1)}\right]^T \in \mathbb{C}^{K\times 1}$: vector noise

Let,

$$R_{n,,q} = \left[r_{n,0,q}, \dots, r_{n,P-1,q}\right]^T \in \mathbb{C}^{K\times 1} \quad (26)$$

$$R_{n,q} = C_n^H x_{n,q} = E_{n,q}\sigma + v'_{n,q} \quad (27)$$

Where,

$r_{n,p,,q}$: modulated echo

$v'_{n,q}$: the noise vectors modified without power change

For each OFDM subcarrier, each transmitter/receiver pair :

$$\varepsilon_{n,p,q}^{(0)} = exp^{\{j2\pi(n\Delta f+f_0)\tau_{p,q}^{(0)}\}},$$

$$\tau_{p,q}^{(0)} = \frac{\|o - Z_p\|\|W_q - o\|}{C} - \tau_{min} \quad (28)$$

$r_{n,p,q}$ is multiplied by $\varepsilon_{n,p,q}^{(0)}$ for a compensated initial phase

$$h_{n,p,q} = \varepsilon_{n,p,q}^{(0)} r_{n,p,q} = \sum_{i=1}^{I} exp^{\{j2\pi(n\Delta f + f_0)(\tau_{p,q}^{(0)} - \tau_{p,q}^{(i)}\}} \sigma_i \; + \tilde{v}_{n,p,q}$$

(29)

$\tilde{v}_{n,p,q}$ is the noise after compensation. Then,

$$\tau_{p,q}^{(0)} - \tau_{p,q}^{(i)} = \frac{\|o - Z_p\| + \|W_q - o\| - \|h_i - Z_p\| - \|W_q - h_i\|}{C}$$

(30)

With,

Z_p the p-th transmitter et W_q the q-th receiver.

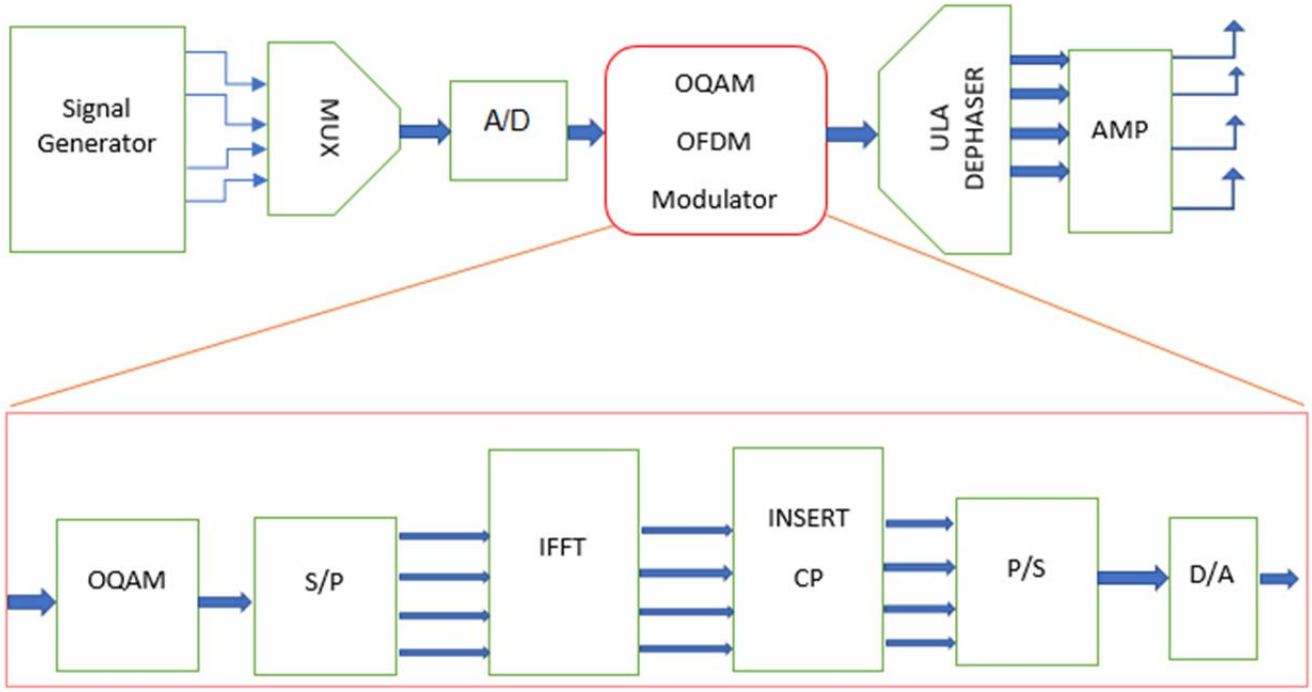

Fig. 4. *OFDM OQAM transmitter for MIMO Radar*

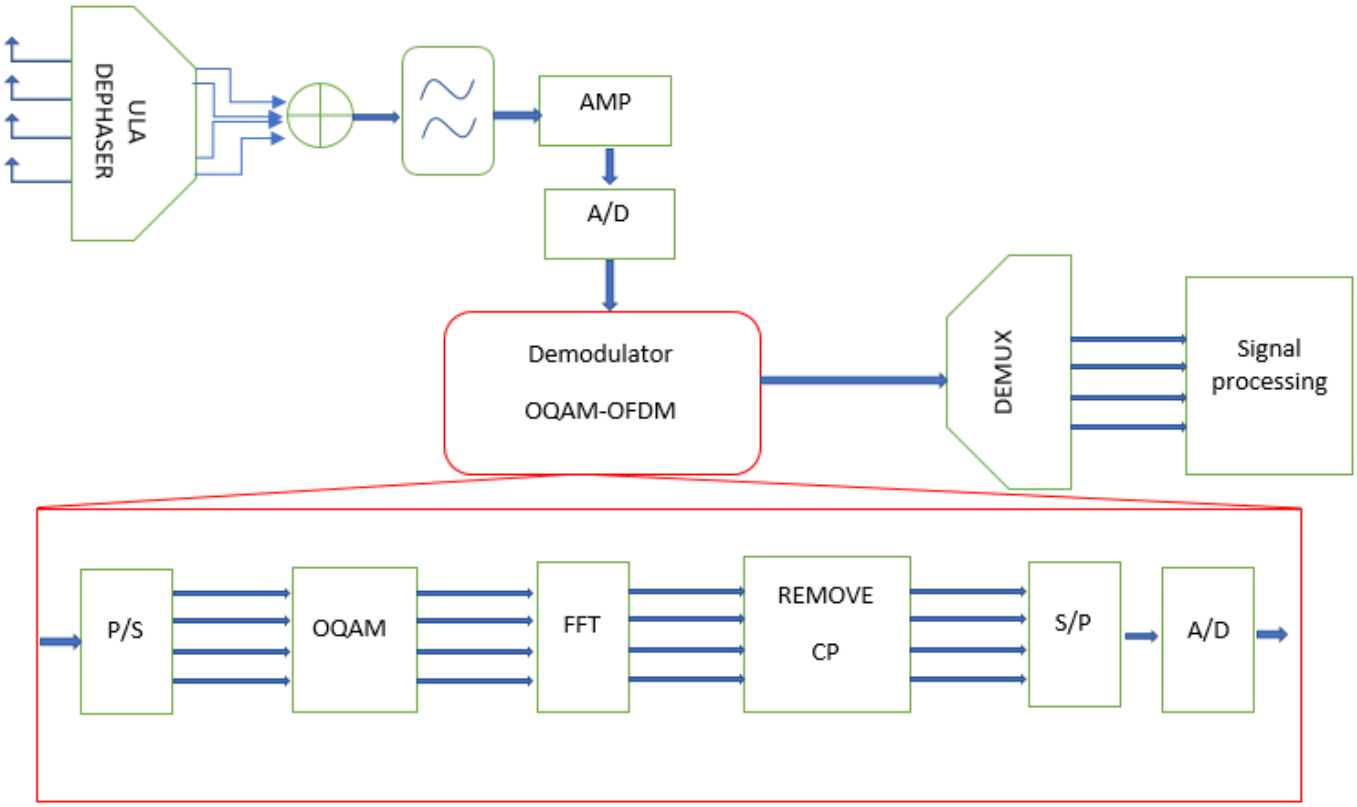

Fig. 5. *OFDM OQAM receiver for MIMO Radar*

The operators in the fig. 4 and fig. 5 are :

- Signal generator : generate binary data to be sent
- MUX : Multiplexing the multiple signals generated to be sent on one channel
- A/D : Analog to digital
- S/P : Serial to Parallel
- IFFT : Inverse Fast Fourier Transform
- CP : Clipping
- ULA dehaser : equation (10)
- AMP : Amplifier
- D/A : Digital to Analog
- P/S : Parallel to Serial
- FFT : Fast Fourier Transform

If $\tilde{\sigma}_i = \sigma_i \exp\{j2\pi \frac{(-2u_i+\mu_i)}{\lambda}\}$ designates the modulated dispersion amplitude phase, which is a constant for a transmitter/receiver chain.

$$\begin{cases} \Delta u = \frac{C}{2N\Delta f} \\ \Delta \tilde{x} = \frac{Cd_0}{Pf_0 d_t} \\ \Delta \tilde{y} = \frac{Cd_0}{Qf_0 d_r} \end{cases} \quad (31)$$

The equation (31) expresses the resolution of the radial distance and the section respectively, with $\lambda_0 = \frac{C}{f_0}$ being the wavelength of the system. Pd_t and Qd_r is the distances between the transmitters, and QD_r is the distance between the receivers.

$$u_i = \bar{h}_i^T d_0 \quad (32)$$

$$\bar{h}_i = h_i - o \quad (33)$$

$$(\tilde{x}_i, \tilde{y}_i, \tilde{z}_i)^T = \bar{h}_i - u_i d_0 \quad (34)$$

$$\mu_i = \left(\bar{h}_i - u_i d_0\right)^T (Z_0 + W_0) \quad (35)$$

With,

u_i : the radial distance

The signal received is therefore expressed by the equation (36).

$$h_{n,p,q} = \varepsilon_{n,p,q}^{(0)} r_{n,p,q} = \sum_{i=1}^{I} \tilde{\sigma}_i . exp^{\{j\pi\omega_{1,i} + jP\omega_{2,i} + jQ\omega_{3,i}\}} + \tilde{v}_{n,p,q} \quad (36)$$

With, $\begin{cases} \omega_{1,i} = \frac{-2\pi\lambda_i}{N\Delta u} \\ \omega_{2,i} = \frac{2\pi\tilde{x}_i}{P\Delta\tilde{x}} \\ \omega_{3,i} = \frac{2\pi\tilde{y}_i}{Q\Delta\tilde{y}} \end{cases}$

After the OFDM theory on transmitter and receiver signal, the OQAM processing could also be applied to it.

On the OQAM-OFDM, the modulated signal will be expressed by the equation (37).

$$x(t) = \sum_{n=0}^{N-1} \frac{1}{\sqrt{N}} exp^{\left(j2\pi\frac{tn}{N}\right)} s_n = V.S \quad (37)$$

N : Number of subcarriers of IDFT

V : Columns of IDFT

S : vector of symbol O-QAM

s_n : symbol OQAM carried by the n-th subcarrier expressed by the equation (38)

$$s_n(t) = \theta_{l,k} . a_{l,k} . \delta(t - k\frac{T_s}{2}) \quad (38)$$

2.4. FBMC-OQAM MIMO radar

FBMC scheme is able to tackle the flaws of OFDM by adding generalized pulse shaping filters that offer a good time and frequency localization properties. FBMC system has more spectral containment and offers more optimization in terms of radio resource utilization as CP is no more required. FBMC system uses filterbanks, on the transmitter and receiver side. The filterbanks consist of an array of many filters that processes many input signals to produce the outputs.

The filter bank at the transmitter side is a synthesis filter bank and the one at the receiver side is an analysis filter bank. The input bitstream is first converted from serial to parallel multiple substreams and then introduced in the synthesis filter bank, converted back to serial bitstream after going out of synthesis bank.

This fig. 6 compares the synthesis filter and analysis filter. The PPN will be the polyphase network filter used on a transmitter and on a receiver.

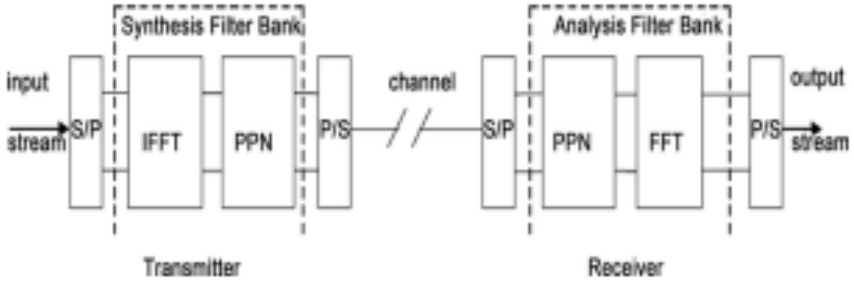

Fig. 6. *OFDM OQAM receiver for MIMO Radar*

On the receiver side, the bit stream is converted from serial to parallel form by the serial-to-parallel converter and moves into the analysis filter bank.

After the OQAM pre-processing, the OQAM symbols are shaped on the different sub-carriers by a bank of synthesis filters. This last ensures the correct localization in time and frequency of these sub-carriers in accordance with the specifications of the prototype filter used. The signal at the output of the synthesis filter bank has the expression in the equation (39).

$$S(t) = \sum_{l=0}^{N-1} \sum_{k=-\infty}^{+\infty} j^{l+k} a_{l,k} h\left(t - k\frac{T_s}{2}\right) e^{j\frac{2\pi l}{T_s}t} \tag{39}$$

Where,

N : number of subcarriers

l : index of frequency

k : index of time

$a_{l,k}$: symbol of OQAM

$h(t)$: The impulse response of the prototype filter is used. The impulse response of a system is the output obtained when the input is an impulse, i.e. a sudden and brief variation of the signal.

The first step in our approach to present this approach is to consider a prototype filter defined by an impulse response whose coefficients h_i connect the input x of the filter to its output y by equation (40) :

$$\boldsymbol{y(k) = \sum_{i=1}^{L_p} h_i . x(k-i)}$$

(40)

Where L is the length of the filter

The frequency response of the filter obtained after the Fourier transform is expressed by the equation (41).

$$\boldsymbol{H(f) = \sum_{i=1}^{L_p} h_i . e^{-j2\pi if}}$$

The Z-transform is obtained by setting $\boldsymbol{e^{j2\pi f} = Z}$. The equation (42) expresses the z-transform of H.

$$\boldsymbol{H(Z) = \sum_{i=1}^{L_p} h_i . Z^{-i}}$$

(42)

Where,

$L_p = KN$

K : overlap factor

N : number of subcarriers

After polyphase decomposition, the filter H(Z) can be decomposed into N elementary filters according to the equation (43) obtained by posing $i = k'N + n'$ where $0 \leq k' \leq K-1$ and $0 \leq n' \leq N-1$

$$H(Z) = \sum_{n'=0}^{N-1} \sum_{k'=0}^{K-1} h_{k'N+n'} . Z^{-(k'N+n')}$$

(43)

$$H(Z) = \sum_{n'=0}^{N-1} \left[\sum_{k'=0}^{K-1} h_{k'N+n'} . Z^{-(k'N)} \right] . Z^{-n'}$$

(44)

Let's pose $E_{n'}(Z^N)$ the n'-th expressed by the equation (45).

$$\boldsymbol{E_{n'}(Z^N) = \sum_{k'=0}^{K-1} h_{k'L+n'} . Z^{-(k'N)}}$$

(45)

After decomposition, the filter will be expressed by the equation (46).

$$\boldsymbol{H(Z) = \sum_{n'=0}^{N-1} E_{n'}(Z^N) . Z^{-n'}}$$

(46)

The synthesis filter bank consists of N shifted versions of the prototype filter. Each version is frequency-centric i/N where I = 0,1,…,N-1 and expressed by the equation (47).

$$\boldsymbol{H_i(Z) = \sum_{n\prime=0}^{N-1} e^{j2\pi n\prime \frac{i}{N}} E_{n\prime}(Z^N).Z^{-n\prime}}$$

(57)

By posing $w = e^{-j\frac{2\pi}{N}}$, the synthesis filter bank can be written in matrix form like expressed in the equation (48).

$$\begin{bmatrix} \boldsymbol{H_0(Z)} \\ \boldsymbol{H_1(Z)} \\ \vdots \\ \boldsymbol{H_{N-1}(Z)} \end{bmatrix} = \begin{bmatrix} \mathbf{1} & \mathbf{1} & \cdots & \mathbf{1} \\ \mathbf{1} & \boldsymbol{w^{-1}} & & \boldsymbol{w^{-(N-1)}} \\ & \vdots & \ddots & \vdots \\ \mathbf{1} & \boldsymbol{w^{-(N-1)}} & \cdots & \boldsymbol{w^{-(N-1)^2}} \end{bmatrix} . \begin{bmatrix} \boldsymbol{E_0(Z^N)} \\ \boldsymbol{E_1(Z^N).Z^{-1}} \\ \vdots \\ \boldsymbol{E_{N-1}(Z^N).Z^{-(N-1)}} \end{bmatrix}$$

(48)

Where, the square matrix is the inverse discrete Fourier transform matrix of order N.

The polyphase realization of the FBMC-OQAM transmitter amounts to the implementation of the emission filter bank (synthesis filter bank) represented by equation (48).

Fig. 7 illustrates the diagram of the synthesis filter bank deduced from equation (47). The polyphase decomposition reduces the complexity of the implementation.

Similarly, with the polyphase of the synthesis filter bank previously, the analysis filter bank has the expression in the equation (49).

$$H_{-i}(Z) = \sum_{n\prime=0}^{N-1} e^{-j2\pi n\prime \frac{i}{N}} E_{n\prime}(Z^N).Z^{-n\prime}$$

(49)

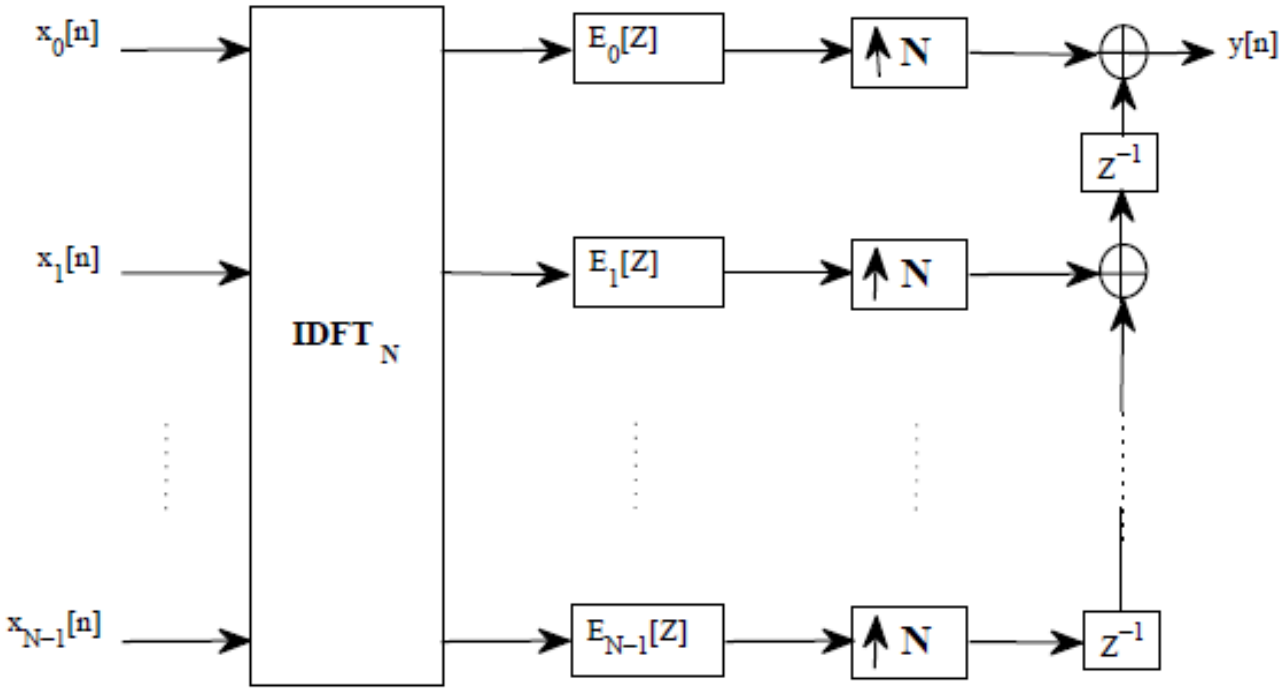

Where, $\uparrow N$:the oversampling operation with the factor N.

Fig. 7. *synthesis filter bank on FBMC*

Let's pose $w = e^{-j\frac{2\pi}{N}}$, the analysis filter bank can be written in matrix form by the equation (50).

$$\begin{bmatrix} H_0(Z) \\ H_1(Z) \\ \vdots \\ H_{N-1}(Z) \end{bmatrix} = \begin{bmatrix} 1 & 1 & \cdots & 1 \\ 1 & w^{-1} & & w^{-(N-1)} \\ & \vdots & \ddots & \vdots \\ 1 & w^{-(N-1)} & \cdots & w^{-(N-1)^2} \end{bmatrix} \cdot \begin{bmatrix} E_0(Z^N) \\ E_1(Z^N).Z^{-1} \\ \vdots \\ E_{N-1}(Z^N).Z^{-(N-1)} \end{bmatrix} \tag{50}$$

Where, the square matrix is the inverse discrete Fourier transform matrix of order N.

The polyphase realization of the FBMC-OQAM receiver amounts to the implementation of the reception filter bank (synthesis filter bank) represented by equation (48).

Fig. 8 illustrates the diagram of the analysis filter bank deduced from equation (50). The polyphase decomposition reduces the complexity of the implementation.

Several types of prototype filters are proposed: rectangular window (for the case of OFDM), Gaussian function, the IOTA filter (Isotropic Orthogonal Transform Algorithm), the PHYDYAS filter (Physical layer for dynamic spectrum access and cognitive Radio, etc.). The PHYDYAS filter is used for FBMC-OQAM.

This filter which owes its name to the European project "PHYsical layer for DYnamic spectrum Access and cognitive radio" was designed by Bellanger in 2001. Its realization consists in determining the frequency coefficients and in building from these coefficients the frequency response and then the impulse response by the inverse Fourier transform.

Determining which filter frequency coefficients are symmetric depends on the overlap factor $K = \frac{Lp}{N}$, where L_p is the number of coefficients of the impulse response of the searched filter and N is the carrier number. Table 1 shows the values of the coefficients of the frequency response of the PHYDYAS filter for K=2,3,4

For K>4, the coefficients are expressed by the equation (51).

$$\begin{cases} H_0 = 1, H_1 = 0.97195983, H_2 = \frac{\sqrt{2}}{2} \\ H_3 = \sqrt{1 - H_1^2}, H_k = 0 \; pour \; 4 < k < L_p - 1 \end{cases} \tag{51}$$

The frequency response is obtained from the frequency coefficients using equation (52).

$$H(f) = \sum_{k=-(K-1)}^{K-1} H_k \frac{\sin\left(\pi\left(f - \frac{k}{NK}\right)NK\right)}{NK\sin\left(\pi\left(f - \frac{k}{NK}\right)\right)} \tag{52}$$

The impulse response is expressed by the equation (52) (it is the Inverse Fourier transform of H(f)).

$$h(t) = 1 + 2\sum_{k=0}^{K-1} H_k \cos\left(2\pi\frac{kt}{KT}\right) \tag{53}$$

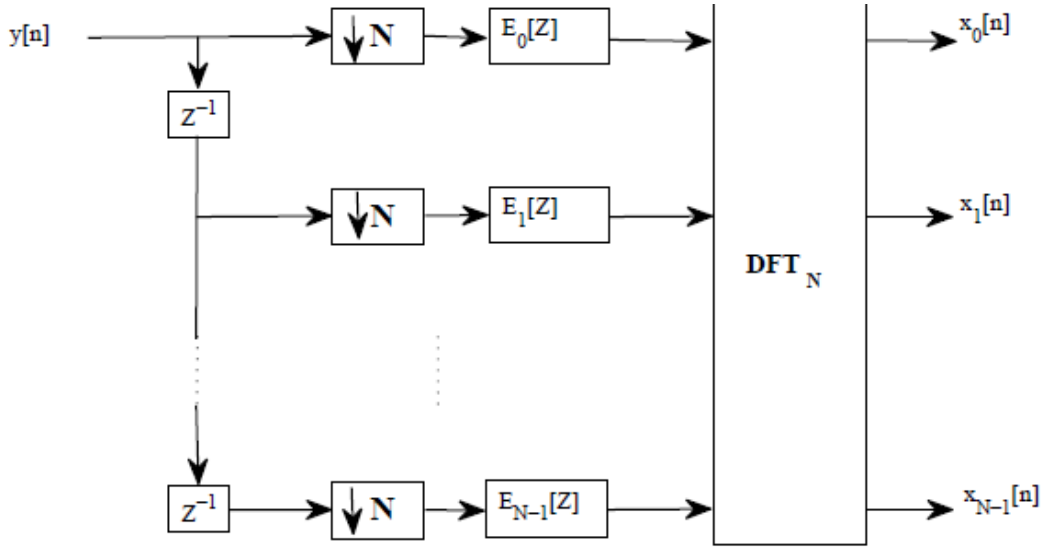

Fig. 8. *Analysis filter bank on FBMC*

TABLE I. THE COEFFICIENTS OF THE FREQUENCY RESPONSE OF THE PHYDYAS FILTER FOR K=2,3,4

K	H_0	H_1	H_2	H_3
2	1	$\frac{\sqrt{2}}{2}$		
3	1	0.911438	0.411438	
4	1	0.971960	$\frac{\sqrt{2}}{2}$	0.235147

2.5. DFT-FBMC

By default the classic trasform used with FBMC is the IDFT in the transmitter and DFT in the receiver. The IDFT could be expressed in the equation (54).

$$x(t) = \sum_{n=0}^{N-1} \frac{1}{\sqrt{N}} exp^{\left(j2\pi\frac{nt}{N}\right)} s_{i,n}(t).g(t-kT) \tag{54}$$

Where,

s_n : Symbol carried by the n-th subcarrier

g : Rectangular function with period T

N : Number of subcarriers of IDFT

To recover the signal, the DFT process should be done as expressed in the equation (55)

$$s_{i,n}(k) = \frac{1}{N}\sum_{k=0}^{N-1} x(k).e^{j\frac{2\pi}{N}k.n} \tag{55}$$

2.6. DCT-FBMC

The IDFT on FBMC could be replace by IDCT which could be expressed by the equation (56).

$$x(t) = \sum_{n=0}^{N-1} \beta_n.\cos\left(\frac{\pi(2t-1)(n-1)}{2.N}\right) s_{i,n}(t).g(t-kT) \tag{56}$$

Where,

s_n : Symbol carried by the n-th subcarrier

g : Rectangular function with period T

N : Number of subcarriers of IDFT

And

$$\beta_n = \begin{cases} \frac{1}{\sqrt{2}} \; if \; n = 0 \\ 1 \; if \; 2 \leq n \leq N-1 \end{cases} \tag{57}$$

To recover the signal, the DCT process should be done as expressed in the equation (58)

$$s_{i,n}(k) = \sqrt{\frac{2}{N}} . \sum_{k=0}^{N-1} x(k) . \beta_k . cos\left(\frac{\pi.(2n-1).(k-1)}{2N}\right) \tag{58}$$

2.7. LWT-FBMC

The IDFT on FBMC could be also replaced by ILWT. The ILWT is defined by a sequence $\{Y(z)\}$, and can be given by the equation (59).

$$y_{ILWT}[t] = \sum_{q=0}^{Q-1}\sum_{n=0}^{N-1}\left(s_{i,n}(t)\right)^{q}.(2)^{\frac{q}{2}}.\psi(2^{q}.t-n) \tag{59}$$

To recover the signal, the LWT process should be done as expressed in the equation (60).

$$s_{LWT}^{q}(z) = \sum_{k=0}^{N-1}(x(k)).2^{\frac{z}{2}}\psi(2^{z}.k-q);\quad z = 0,1,2,\dots,N-1\ and\ q = 0,1,2,\dots,N-1 \tag{60}$$

An alternative method for constructing the biorthogonal wavelet transform, the lifting scheme in fig. 9 and fig. 10, has some advantages over the classical standard wavelet transform which are given below.

- It is a spatial domain method,
- It is easy to use for implementation,
- It allows the use of quicker and in-place computations,
- It allows the use of nonlinear, adaptable, disorderedly sampled and integer to integer wavelet transforms,

Another advantage of the lifting scheme is that the LWT and the reverse-LWT shown in fig. 9 and fig. 10 are completely symmetrical to each other. This ensures that LWT can be applied easily.

Filters and subsampling are used in traditional wavelet transform processes. The lifting method was developed by Sweldens in 1992 to reduce the complex mathematical operations used in filtering. The lifting method is the simplest and most efficient method for wavelet transformation.

In the lifting method, the signal is divided into odd and even samples. Instead of filters, Spit Predit and Update processes are applied. Complex calculations are not required for these operations as in traditional methods.

In the figure, U means *Update*, P means *Prediction*, S means *Spit* and M means *Merge*.

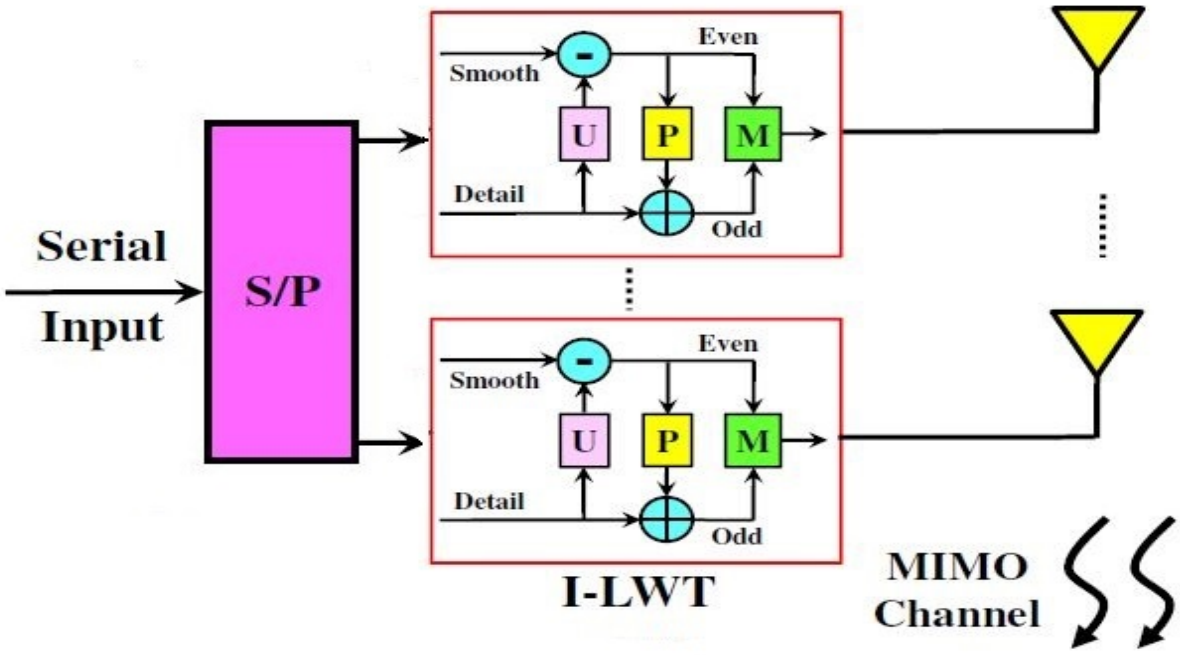

Fig. 9. *Fast computation ILWT*

The original X[k] signal is primarily separated into odd and even components, as in the equations (61) and (62).

$$X_{odd}[k] = X[2k+1] \tag{61}$$

$$X_{even}[k] = X[2k] \tag{62}$$

There is a strong correlation between these two examples. In the predict step, odd samples are tried to be obtained approximately by making use of even samples. The second part, Predict, preserves the high frequency components by eliminating the low frequency components of the signal. In the prediction process, the subset $X_{odd}[k]$ is predicted over the subset $X_{even}[k]$ using the prediction operator P(.). The detail information of the X[k] signal is obtained as in equation (63) by taking the difference between the subset $X_{odd}[k]$ and the predicted P($X_{even}[k]$). The P(.) Prediction operator is a linear combination of a single neighboring subset.

$$P(X_{even}[k]) = \sum_i (p_i . X_{even}[k+i]) \tag{63}$$

Here, p_i are the prediction coefficients. This step acts as a high pass filter and the high frequency components (d[k]) that give the detail part of the obtained signal.

$$d[k] = X_{odd}[k] - P(X_{even}[k]) \tag{64}$$

After calculating the prediction p_i,

$$d[k] = d[2y+1] = \begin{cases} X[2y+1] - \frac{X[2y]+X[2y+2]}{2} & Normal \\ X[2y+1] - X[2y] & 0dd\ end \end{cases} \tag{65}$$

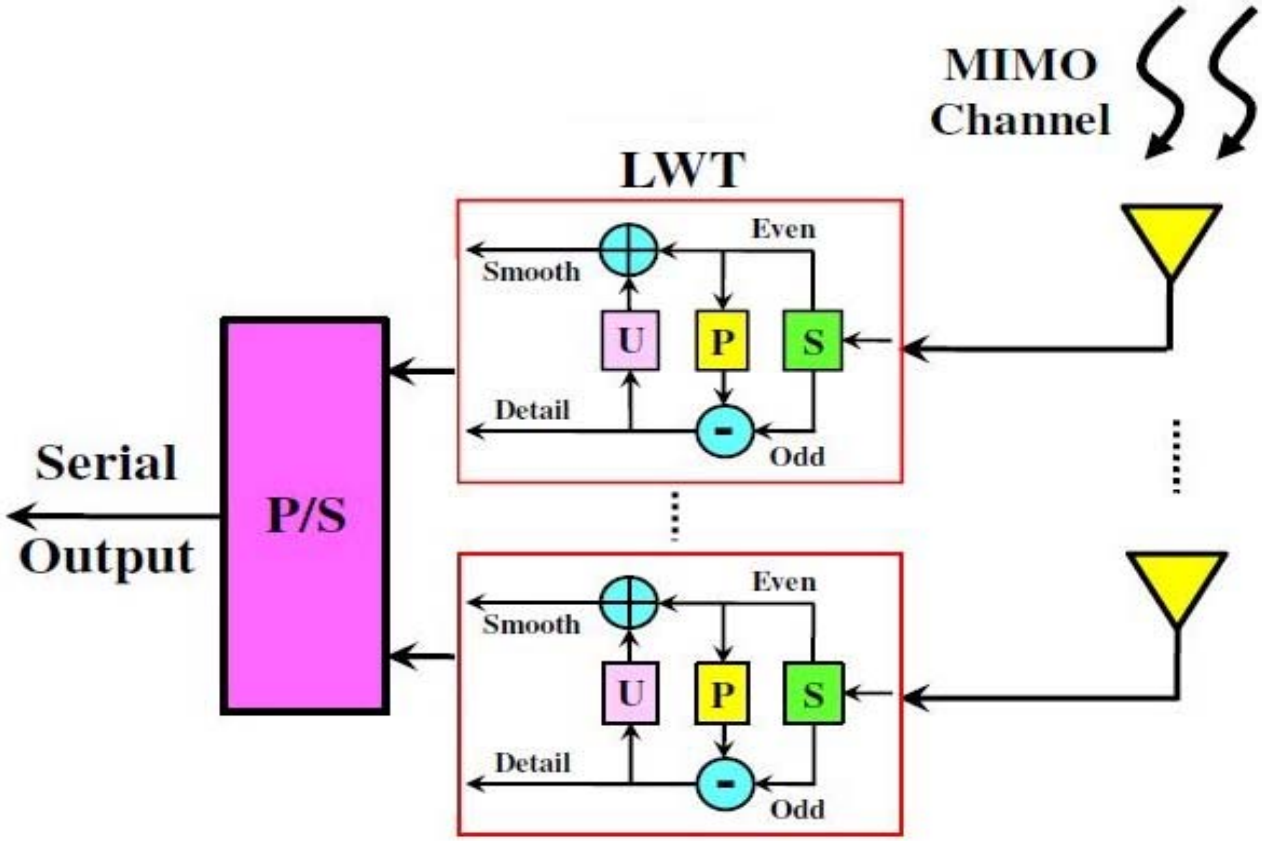

Fig. 10. *Fast computation LWT*

In the update step, the samples are scaled to fix and then added with even samples to provide low pass filtered values for transformation. In the third part, update, the even components are updated by using the detailed signal to reduce the frequency aliasing effect.

In the update process, the approximate information about the signal is obtained as a result of collecting the detailed information entering the U(.) Update operator with the subset $X_{even}[k]]$. The U(.) Update operator is a linear combination of neighboring d[k] values. The formula for the U(.) Update operator is specified in equation (66).

$$U(d[k]) = \sum_i (u_i d[k+i]) \tag{66}$$

Here, u_i are the updating coefficients. In the update process, the approximate value of the obtained signal by passing the signal through a low pass filter is obtained by updating the linear combination of the d[k] prediction difference as in the equation (67). These examples contain low frequency components that give approximate information (s[k]) about the signal.

$$s[k] = X_{even}[k] + U(d[k]) \tag{67}$$

After calculating the prediction u_i,

$$s[k] = s[2y] = \begin{cases} X[2y] + \frac{V[2y+1]+1}{2} & Normal \\ X[2y] + \frac{X[2y-1]-X[2y]+1}{2} & Even\ end \end{cases} \tag{68}$$

Inverse transformation is obtained by applying the exact opposite operations used in the conversion to the obtained d[k] and s[k] signals. Inverse Lifting wavelet transformation is given in fig. 9 in I-LWT block in detail.

$$X_{odd}[k] = d[k] + P(X_{even}[k]) \tag{69}$$

$$X_{even}[k] = s[k] - U(d[k]) \tag{70}$$

After the inverse transformation process, as given in equation (71), the original signal is obtained by combining the odd index and even index samples with the MRG combination operator.

$$X[k] = MRG\{X_{odd}[k], X_{even}[k]\} \tag{71}$$

The equations (64) and (67) could be performed using the matrix form expressed in the equation (72).

$$\begin{bmatrix} d[k] \\ s[k] \end{bmatrix} = \begin{bmatrix} 1 & -P(.) \\ U(.) & 1-P(.)U(.) \end{bmatrix} \cdot \begin{bmatrix} X_{odd}[k] \\ X_{even}[k] \end{bmatrix} = A. \begin{bmatrix} X_{odd}[k] \\ X_{even}[k] \end{bmatrix} \tag{72}$$

With,

$$A = \begin{bmatrix} 1 & -P(.) \\ U(.) & 1-P(.)U(.) \end{bmatrix} \tag{73}$$

For the ILWT, the equations (69) and (70) could be simplified using the matrix form expressed in the equation (74) :

$$\begin{bmatrix} X_{odd}[k] \\ X_{even}[k] \end{bmatrix} = \begin{bmatrix} 1-P(.)U(.) & P(.) \\ -U(.) & 1 \end{bmatrix} \cdot \begin{bmatrix} d[k] \\ s[k] \end{bmatrix} = A^{-1} \cdot \begin{bmatrix} d[k] \\ s[k] \end{bmatrix} = A.A. \begin{bmatrix} d[k] \\ s[k] \end{bmatrix} \tag{74}$$

With,

$$A^{-1} = A.A = \begin{bmatrix} 1-P(.)U(.) & P(.) \\ -U(.) & 1 \end{bmatrix} \tag{75}$$

2.8. Mutliple Transforms with FBMC

The Inverse Multiple Transform (IMT) with N carriers could be : IDFT, IDCT, ILWT in transmitter like in the fig. 11.

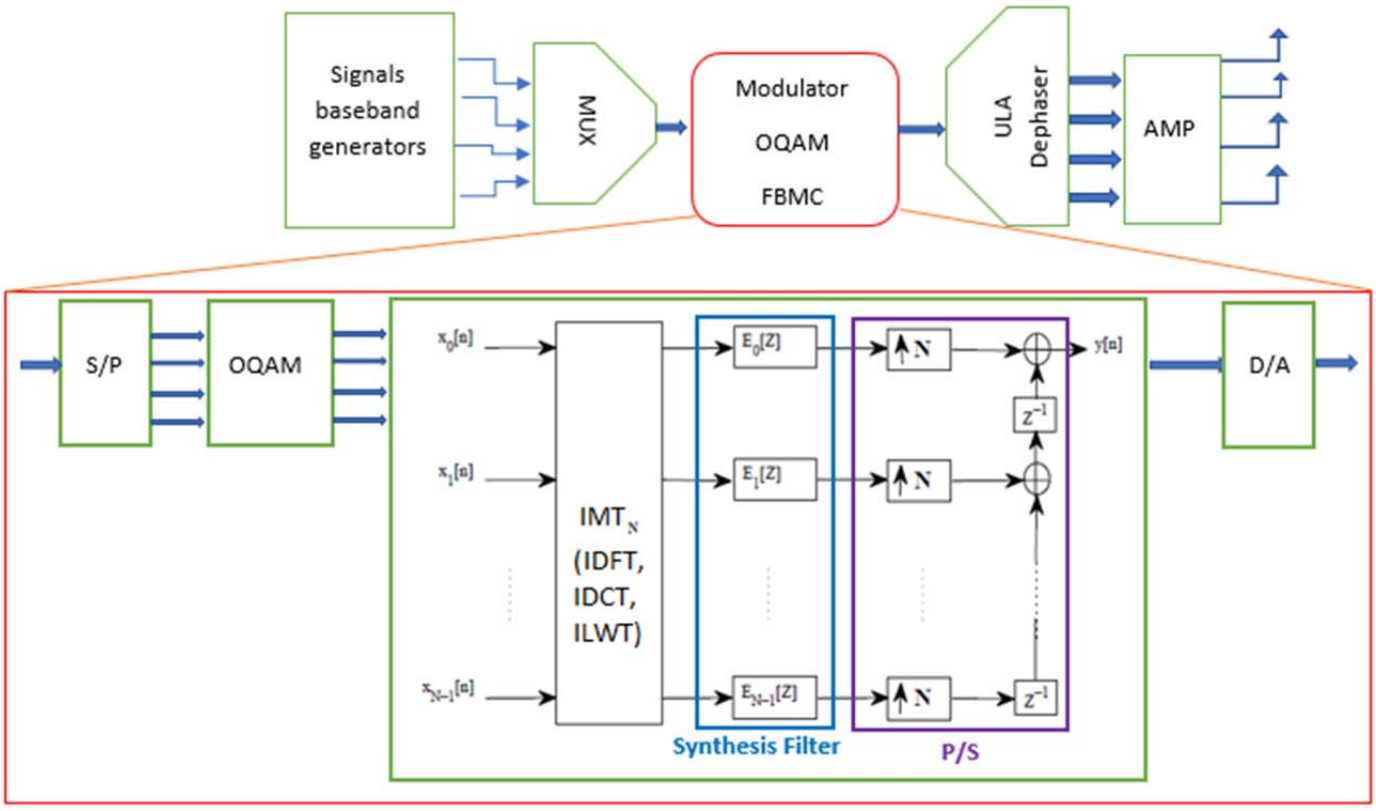

Fig. 11. *FBMC OQAM transmitter with Inverse Multiple Transform (IDFT, IDCT, ILWT)*

On the receiver, the Multiple Transform (MT) should be applied like DFT, DCT and LWT to reconstruct the signal in the fig. 12.

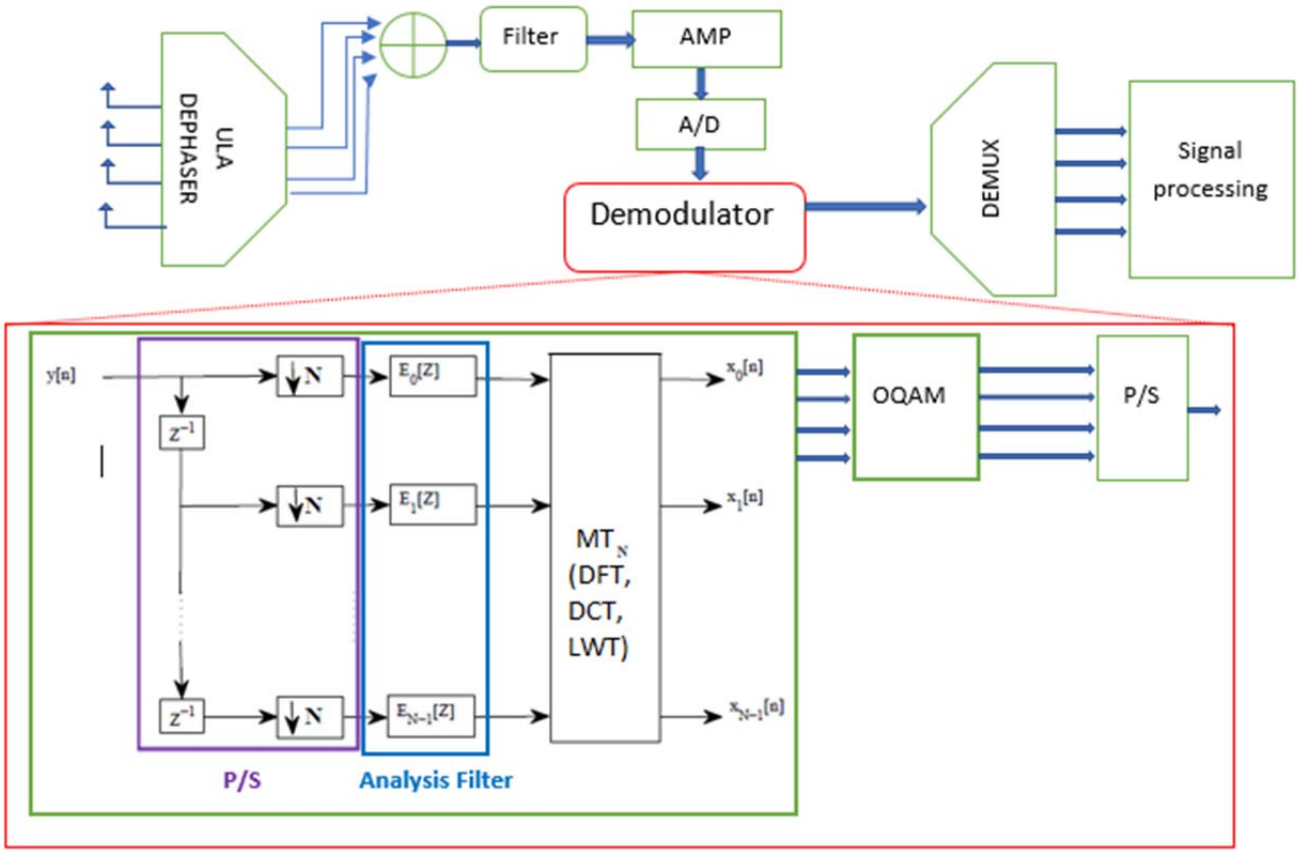

Fig. 12. *FBMC OQAM receiver with Multiple Transform (DFT, DCT, LWT)*

III. RESULTS AND DISCUSSIONS

3.1. Power Spectrum Density

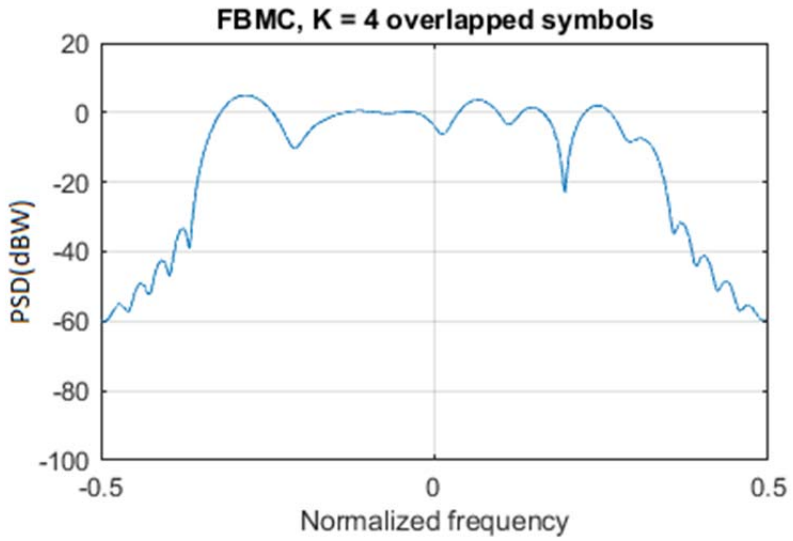

Fig. 13. *Power spectrum density of modulated signal using FBMC-OQAM with IDFT*

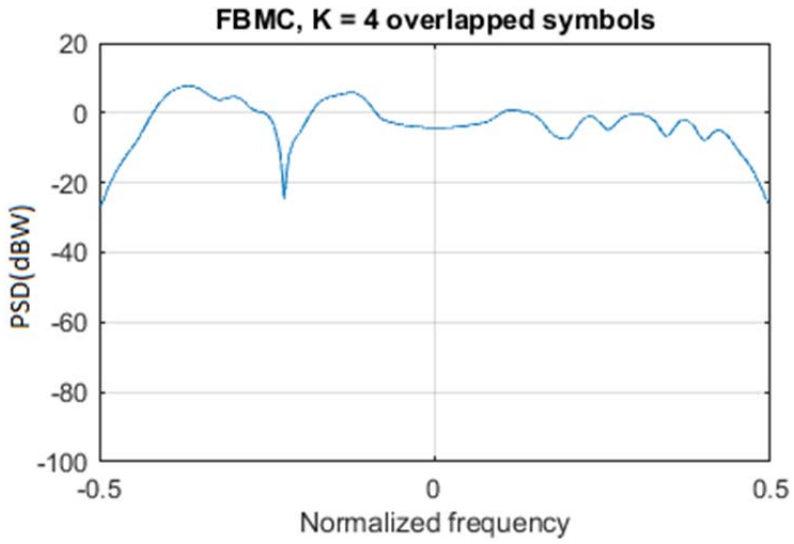

Fig. 14. *Power spectrum density of modulated signal using FBMC-OQAM with IDCT*

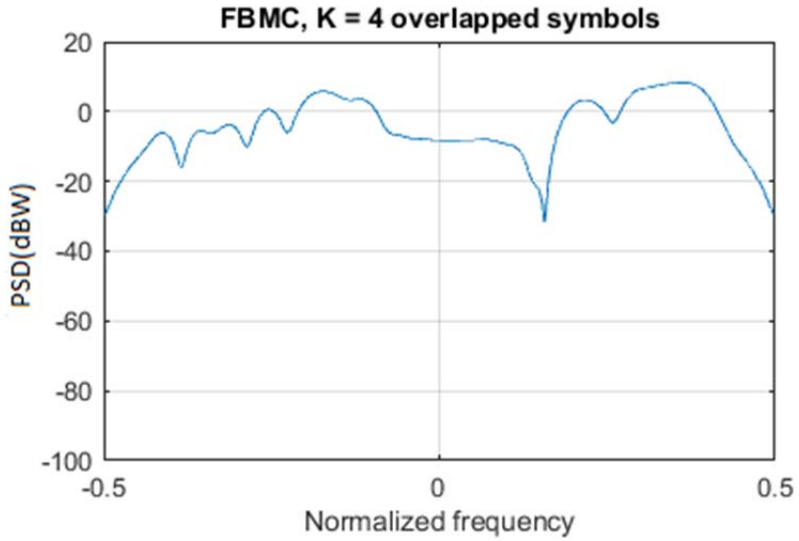

Fig. 15. *Power spectrum density of modulated signal using FBMC-OQAM with ILWT*

The three fig. 13,14,15 give the spectrum of modulated signal using Inverse Multiple Transform with FBMC. The classic IDFT shows that it has more spectrum efficient than the IDCT and ILWT. But, the difference it's not so big indeed between IDFT-FBMC and IDCT-FBMC. Due to interpolation of ILWT, The ILWT-FBMC is not so orthogonal. So the interference between the multi-carriers should be large. Even IDCT has this problem.

We don't vary the number of sub-carries. When the sub-carries are big, the two modulations could give a same performance. So, this result with 4 sub-carries gives us the worst case for spectrum analyzer.

Due to the filter bank on the transmitter, the FBMC has a good filter, so the out of band is as minimal as possible and not seen in the three figures. The power spectrum analyzer is obtained after the full schema bloc of FBMC on fig.11 by changing IMT respectively to IDFT, IDCT and ILWT.

A. Modulated signal

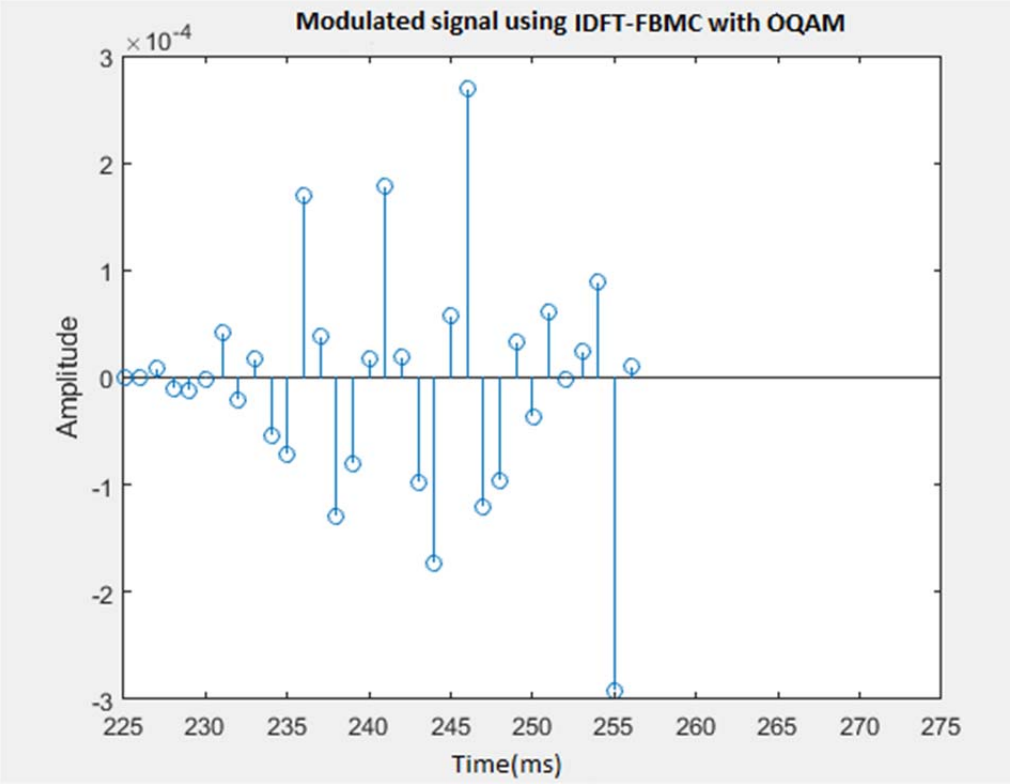

Fig. 16. *modulated signal using FBMC-OQAM with IDFT*

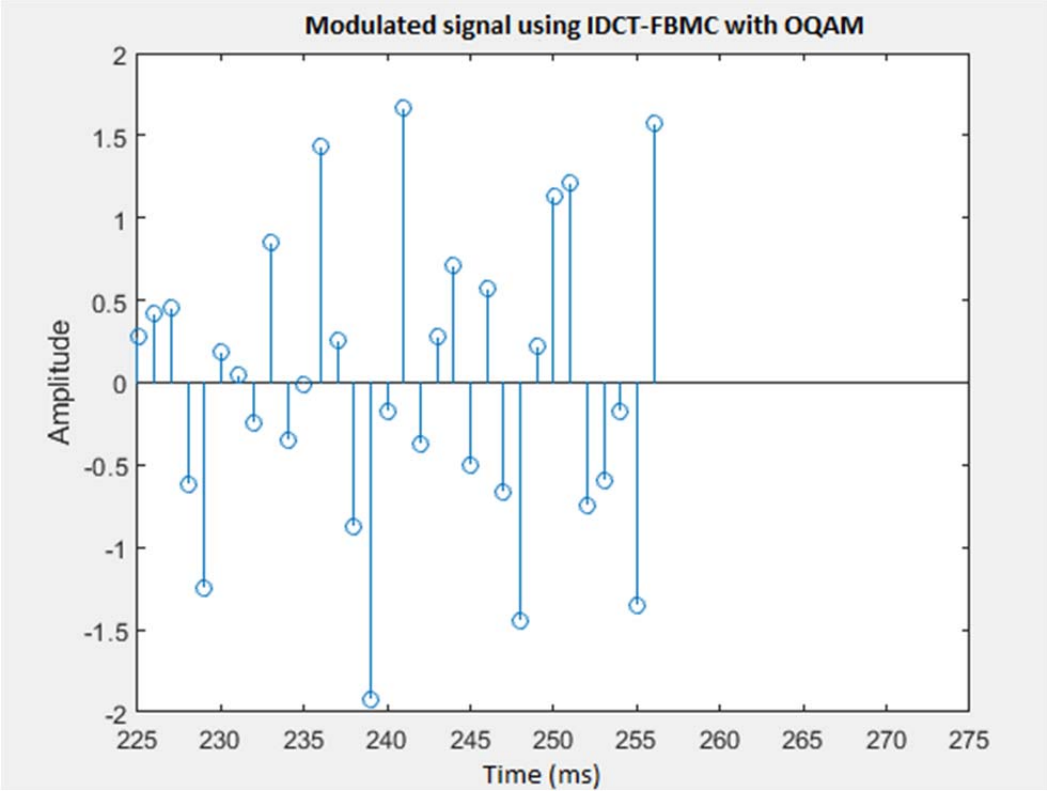

Fig. 17. *modulated signal using FBMC-OQAM with IDCT*

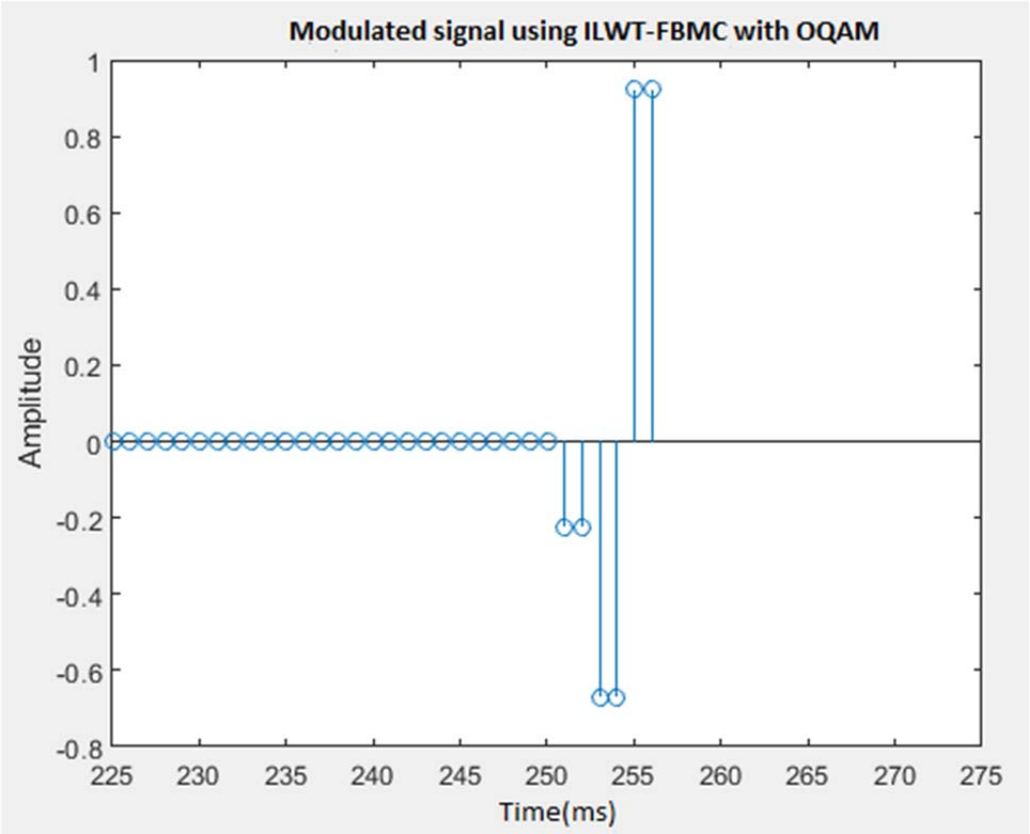

Fig. 18. *modulated signal using FBMC-OQAM with ILWT*

The fig 16,17,18 is a representation of modulated singal of FBMC using respectively IDFT, IDCT and ILWT. The fig.18 could be interpret as the advantage of the ILWT. This transform doesn't present of a big variation on the signal. The transformation combined the detailles information and the smooth information to having a modulated signal like in fig18.

About the two figure based on exponential formula of IDFT and IDCT, the modulated signal presents a big variation on amplitude. It's not very good for the amplifier. Energy will be lost as thermal dissipation and the two schema has a big power consumption than the ILWT.

B. PAPR of the multiple transform

As the interpretation of the modulated signal, the Peak Average Power Ratio shows in fig. 19 that ILWT presents a very low PAPR. With the same power of power amplifier, the ILWT-FBMC could achieve more distance than the others. Indeed, also, the ILWT uses a quick computational using biorthognal interpolation which is obtained by just addition and substraction, just like in the equation 65, 68, 72, 74.

The IDFT and IDCT should use exponential forms and need infinite computation of polynom interpolation. So, the ILWT-FBMC also doesn't spend more power than the IDFT-FBMC and IDCT-FBMC.

The first implementation of multi-carrier modulation using IDF, IDCT, has a very bad PAPR. Some techniques like PAPR reduction and pre-distorsion could improve this problem of power consumption. In this article, we can see that ILWT-FBMC doesn't need another block of PAPR reduction because the wavelet transform reduces this by default.So, with the same power, the ILWT-FBMC could achieve, longer range than IDC-FBMC and IDFT-FBMC which is very useful in the RADAR MIMO.

After the simulation, the ILWT is the best option for PAPR reduction using FBMC modulation instead of IDCT and IDFT when we do 8 tests. But, the technique has also some disadvantages, like the power spectrum not being used more and the bit error ratio being more larger.

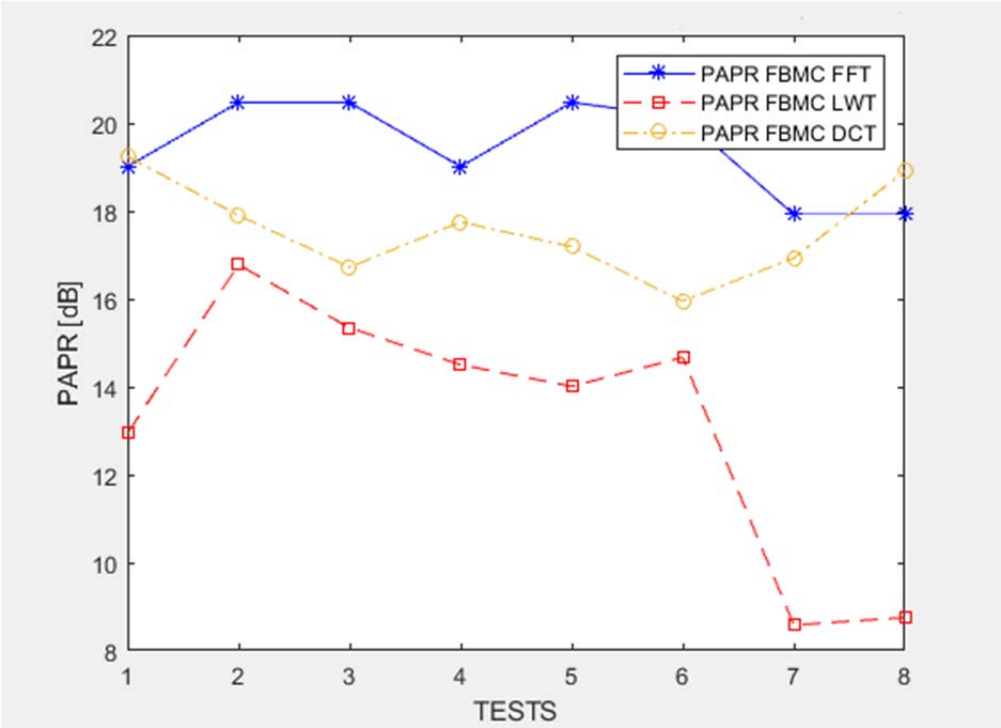

Fig. 19. *PAPR of FBMC-OQAM with Inverse Multiple Transform (IDFT, IDCT, ILWT)*

C. BER of the multiple transform

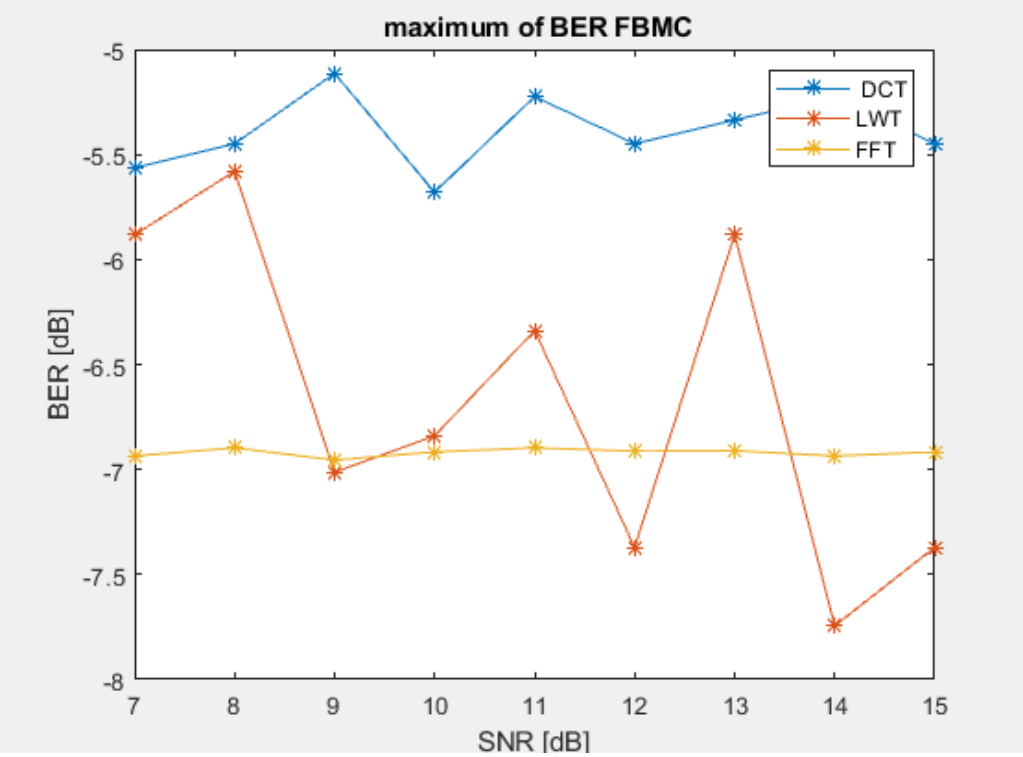

Fig. 20. *BER of FBMC-OQAM with Inverse Multiple Transform (IDFT, IDCT, ILWT)*

The fig.11 and fig. 12 are a complete transmission chain using FBMC with multiple transforms.

So, it's possible to compare the signal to be sent and the signal received and compare the number of bit errors. This number of bit errors is divided by the total number of bits by having a Bit Error Ratio (BER). On the fig. 18 and 19, the BER of FBMC-FFT is a bit similar to FBMC-LWT and the DCT is not more suitable for FBMC modulation.

IV. CONCLUSIONS

As conclusion, FBMC-ILWT gives a good power consumption with MIMO-RADAR. The wavelet transform is very quick and has a less PAPR. The FBMC-IDCT is the second choice but it's not have a quick time processing. For having high data rate, the FBMC-ILWT should use a good code corrector error to resolve the problem about Bit Error Ratio (BER). This proposition is not so useful on RADAR MIMO due less data rate transmitted on it.

REFERENCES

[1]. Zhou, Zhenlei, Lin, Bangjiang, Tang, Xuan, Chaudhary, Sushank, Lin, Chun, "Performance comparison of DFT-OFDM, DCT-OFDM, and DWT-OFDM for visible light communications", spie. Journal, International Conference on Optical Communications and Networks, 2018, Zuhai China.

[2]. Javaid A. Sheikh, Farhana Mustafa, Arshid Iqbal "Resource Allocation of Power in FBMC based 5G Networks using Fuzzy Rule Base System and Wavelet Transform", International Journal of Advanced Research in Science and Engineering (IJARSE), march 2018.

[3]. Zainab Hdeib Al-Shably, Zahir M. Hussain, "Performance of FFT-OFDM versus DWT-OFDM under Compressive Sensing", Journal of Physics: Conference Series, 2021

[4]. Khaizuran Abdullah, Zahir M. Hussain, "Studies on DWT-OFDM and FFT-OFDM Systems", International Conference on Communication, Computer and Power (ICCCP 2009)

[5]. Elif Büşra Tuna, Yusuf İslam Tek, Ali Ozen, "A Novel Approach based on Lifting Wavelet Transform for MIMO-OFDM Systems", Research square 2021

[6]. Sheela M. S., Sukera T. P., Arjun K. R., "Comparaison of FFT-OFDM and DWT-OFDM System in Digital Communication", International Journal of Engineering Research and Technology, IJERT 2018

[7]. Meryem Maras, Elif Nur Ayvaz, Meltem Gömeç, Asuman Sava¸scıhabes, Ali Özen, "A Novel GFDM Waveform Design Based on Cascaded WHT-LWT Transform for the Beyond 5G Wireless Communications", MDPI 2021

[8]. Shanlin wei, Hui li, Wenjie Zhang, Wei Cheng, "A comprehensive performance evaluation of Universal Filtered Mutli-Carrier Technique"

[9]. Zahraa Abdel Hamid, Fathl E. Abd El Samie, "FFT/DWT/DCT OFDM channel estimation using EM algorithm in the presence of chaotic interleaving", IEEE 2012

[10]. Mitali Sahu, Meha Shrivastava, Abhishek Agwekar, "Review of PAPR reduction for MIMO-OFDM Radar with DWT and DCT Multiple Contrainsts", International Journal of Engineering Research and Technology, IJERT 2019.

[11]. B.Prasanna Lakshmi, K.Govinda Rajulu, "DWT based barcode modulation for efficient and secure data transmission through DPSK-OFDM"International Research Journal of Engineering and Technology, IRJET, 2017

[12]. Enggar Fransiska DW, Octarina Nur Samijayan, J Suci Rahmatia, "Design and Performance Investigation of Discrete Wavelet Transform (DWT) Based OFDM using 4-PAM for Indoor VLC System", International Conference on Information and Communication Technology, ICoICT 2019

[13]. Ch.Gangadhar, Md. Habibulla, "Spectral Efficiency Enhancement Through Wavelet Transform Filter Bank for Future Mobile Communications", International Journal of Innovative Technology and Exploring Engineering, IJITEE 2019

[14]. Elif Nur Ayvaz, Meryem Maras, Meltem G¨omec, Asuman Savas¸cıhabes, Ali Ozen, "A Novel Concatenated LWT and WHT Based UFMC Waveform Design for the Next Generation Wireless Communication Systems" IEEJ TRANSACTIONS ON ELECTRICAL AND ELECTRONIC ENGINEERING, 2021

[15]. Engin ÖKSÜZ, Ahmet ALTUN, Büşra ÜLGERLİ, Gökay YÜCEL, Ali ÖZEN, "A Comparative Performance Analyses of FFT Based OFDM and DWT Based OFDM Systems", journal of new result in science, JNRS 2016

[16]. Simmi Garg, Anuj Kumar Sharma, Anand Kumar Tyagi, "Performance Comparison of Proposed Scheme Coded DWT-OFDM System with that of Conventional OFDM", Journal of Unversity of Shanghai for Science and Technology, 2020

[17]. Manjunatha K, Reshma M, "Comparative Study on DWT-OFDM and FFT-OFDM Simulation Using Matlab Simulink", International Journal of Engineering Trends and Technology, IJETT, 2017

[18]. Wim Sweldens, "The Lifting Scheme: A New Philosophy in Biorthogonal Wavelet Constructions", Department of Computer Science